

Production of in situ Vanadium Carbide Particulate Reinforced Iron Matrix Composite

Jing WANG¹, Sijing FU^{2*}

¹ Key Laboratory of Mould & Die Technology of Sichuan Province Universities, Chengdu Technological University, Chengdu 611730, China

² Department of Mechanical Engineering, Chengdu Technological University, Chengdu 611730, China

crossref <http://dx.doi.org/10.5755/j01.ms.20.4.6445>

Received 13 February 2014; accepted 22 July 2014

Vanadium carbide (VC) particulate reinforced Fe-based composite was produced using in situ synthesis technique. The effect of sintering temperature on the densification of Fe-VC composite was investigated. The wear resistance of Fe-VC composite was evaluated using pin-on-disk tests. The phases of Fe-VC composite were determined by X-ray diffraction analysis, and the microstructure of Fe-VC composite was characterized by scanning electron microscopy and transmission electron microscopy. The results show that the optimal sintering temperature is 1473 K; Fe-VC composite consists of VC phase and α -Fe phase; fine spherical VC particles distribute uniformly in iron matrix; and the composite possesses great wear-resistance.

Keywords: Fe-VC composite; microstructure; in situ synthesis; wear.

1. INTRODUCTION

Particle reinforced iron matrix composites have attracted increasing attention in recent years as their good performance such as high specific strength, high specific modulus, high wear resistance and high temperature resistance, has been revealed [1–2]. The production methods of metal matrix composite have mechanical alloying or milling [3–4], powder metallurgy [5–6], stir casting [7], etc. Among these methods, processes for preparing particle reinforced iron matrix composites are mainly powder metallurgy and in situ synthesis technique. The advantages of powder metallurgy technique are: the process is simple and flexible, and the volume fraction of the particle reinforcement can be accurately adjusted in a wide range [8]. The disadvantage of powder metallurgy technique is contaminated matrix-reinforcement interfaces [9]. However, the disadvantage can be avoided if in situ synthesis technique is used to fabricate particle reinforced iron matrix composites. Because the advantages of in situ synthesis technique are: particle reinforcement is fine and thermodynamic stable, the interface between the matrix and the reinforcement is no pollution and the bonding strength of interface is high [10].

In particle reinforced iron matrix composites, the particle reinforcements often used are carbide, nitride and oxide. Among the particle reinforcements, a lot of research is focused on TiC particle reinforced iron matrix composites [11–14]. Few studies have reported Fe-VC surface composites [15–16]. However, there is no report on fabricating bulk Fe-VC composite, in which VC particulates are synthesized in situ. Vanadium carbide (VC), high hardness and good wettability with iron matrix [15], can be expected to fabricate iron matrix composite and to improve the abrasion resistance of iron matrix composite. In this

work, a process, which is regarded as the combination of in situ synthesis technique and powder metallurgy technique and has both in situ synthesis and powder metallurgy technique priority, is used to prepare bulk Fe-VC composite in which VC reinforcement is generated through the reaction: $\text{FeV} + \text{C} = \text{VC} + \text{Fe}$. The aim of this study is to investigate the microstructure and wear properties of the Fe-VC composite.

2. EXPERIMENTAL

For preparing Fe-VC composite, the raw materials used were Fe powders (25 μm), Fe-50wt%V powders (48 μm), Fe-70wt%Cr powders (48 μm), Fe-50wt%Mo powders (48 μm) and carbon black powders (25 μm). Table 1 gave the nominal composition of Fe-VC composite. The process conditions for preparing green compacts of Fe-VC composite were the same as that published in our team earlier work [17]. The dimension of green compact was 20 mm diameter and 35 mm height, and the density of green compact was 70 % of the theoretical density. The green compacts were sintered in a vacuum sintering furnace. The sintering temperature was 1433K, 1473K, 1493K and holding time was 1 hour.

Table 1. The chemical composition of Fe-VC composite

Elements	V	C	Mo	Cr	Fe
Wt(%)	28.3	6.7	2	2	Balance

The bending strength was measured using electromechanical universal testing machine. The dimension of the specimens was 20 mm \times 4 mm \times 2 mm. The bending strength was calculated according the following formula [18].

$$\sigma_F = 3Fl / (2bh^2), \quad (1)$$

where F was the applied normal load, l was the span, b and h were the specimen width and the specimen depth,

* Corresponding author. Tel.: +86-28-87992363, fax: +86-28-87992363. E-mail address: fusijing4129@163.com (K. Locharoenrat)

respectively. The span used was 16 mm and the load speed was 0.1 mm/min.

Dry-sliding abrasive behavior of Fe-VC composite was evaluated using a pin-on-disk test machine. The dimension of the pin was 10 mm diameter and 25 mm height. The outside diameter of the disk was 60 mm, and rotational speed of the disk was 400 rev min⁻¹. The normal load applied between the pin and the disk was 50 N. The total sliding distance was 500 m. All tests were done in air at room temperature. Before each wear test, a fresh 150 grit Al₂O₃ sandpaper was stuck to the disk. Fe-VC composite and hardened 1045 steel were used to make the pins and perform dry-sliding abrasive wear tests, and the hardened 1045 steel was contrast. The weight loss of two materials was weighed using electronic balance and its measure precision was 0.1 mg.

The phase structure and microstructure of Fe-VC composite were examined by using X-ray diffraction (XRD), scanning electron microscopy (SEM) equipped with energy dispersive spectrum (EDS) analysis and transmission electron microscopy (TEM). The wear surfaces of Fe-VC composite and hardened 1045 steel were also characterized by using SEM.

3. RESULTS AND DISCUSSION

3. 1. Phase identification of Fe-VC composite

The Gibbs free energy curves of the reactions ($\text{Fe} + \text{C} = \text{Fe}_3\text{C}$, $\text{V} + \text{C} = \text{VC}$) are shown in Fig. 1. It can be seen that the ΔG^0 for the reaction ($\text{V} + \text{C} = \text{VC}$) is below zero, indicating the reaction can spontaneously carry out in thermodynamics. In addition, the ΔG^0 for the reaction ($\text{V} + \text{C} = \text{VC}$) is far below the reaction ($\text{Fe} + \text{C} = \text{Fe}_3\text{C}$), which indicates the formation of VC is easier than Fe₃C.

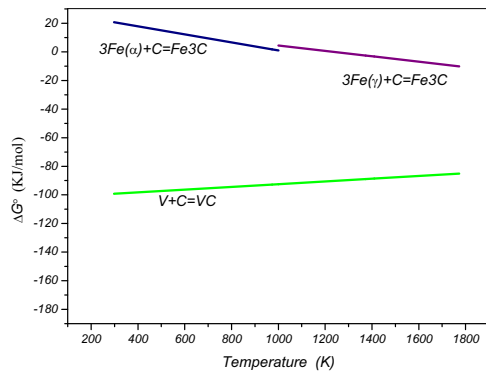


Fig. 1. The Gibbs free energy curves in Fe-V-C system

Fig. 2 and Fig. 3 show the X-ray diffraction spectra of initial powder mixture and Fe-VC composite sintered at 1473 K, respectively. It can be seen that the phases of initial powder mixture are α -Fe, FeV (σ) and C (graphite) (see Fig. 2), and Fe-VC composite consists of VC and α -Fe phases (see Fig. 3), indicating that FeV reacts with C in composite and VC reinforcement forms.

3. 2. Microstructure of Fe-VC composite

Micrographs of the Fe-VC composite sintered at different temperature are presented in Fig. 4, a–c, respectively. The gray regions are VC particles, the lighter areas are iron matrix and the dark spots are voids. It

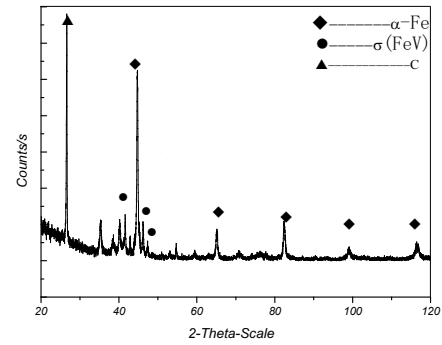


Fig. 2. X-ray diffraction pattern of initial powder mixture

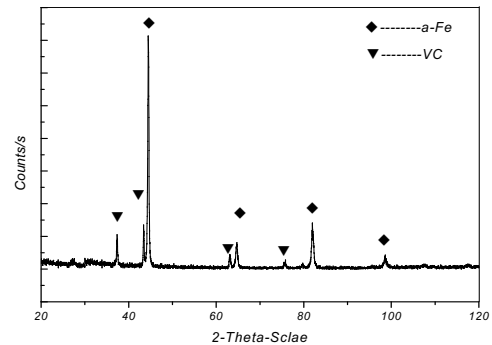


Fig. 3. X-ray diffraction pattern of Fe-VC composite sintered at 1473K

can be found that as sintering temperature enhances, on one hand, the size of the VC particles increases, on the other hand, the voids decrease, reaching a minimum for the composite sintered at 1473 K, after which the voids increasing. There are two main reasons for explaining the phenomenon. One reason is because the liquid metal content in Fe-VC composite increases and the wettability between VC particles and liquid metal is improved as sintering temperature rising, which can cause the voids to decrease. The other reason is that severe volatilization of liquid metal occurs when the sintering temperature is beyond 1473 K. As a result, new voids form and the amount of the voids increases.

In addition, it can also be found that obtaining a pore-free Fe-VC composite is difficult. One important reason is because in order to prepare a pore-free Fe-VC composite, the liquid phase amount and the the density of green compact should match the following condition [19]:

$$f_l^{\min} = \varepsilon_0 \frac{1 - X_i^L}{X_i^L + \varepsilon_0(1 - X_i^L)}, \quad (2)$$

where ε_0 is the initial porosity, and X_i^L is the solubility of element i in the liquid.

In the work, the density of green compact is 0.7 g/cm³, the required solubility of VC in the liquid phase is 0.23~0.41 based on the formula in order to reach a fully dense Fe-VC composite. However, the actual solubility is 0.0135. This demands the density of green compact has to be 0.985~0.993, which is impossible for green compact pressed by traditional powder metallurgy technique.

Fig. 5, a, shows the micrograph of the Fe-VC composite sintered at 1473 K. The gray particles and the

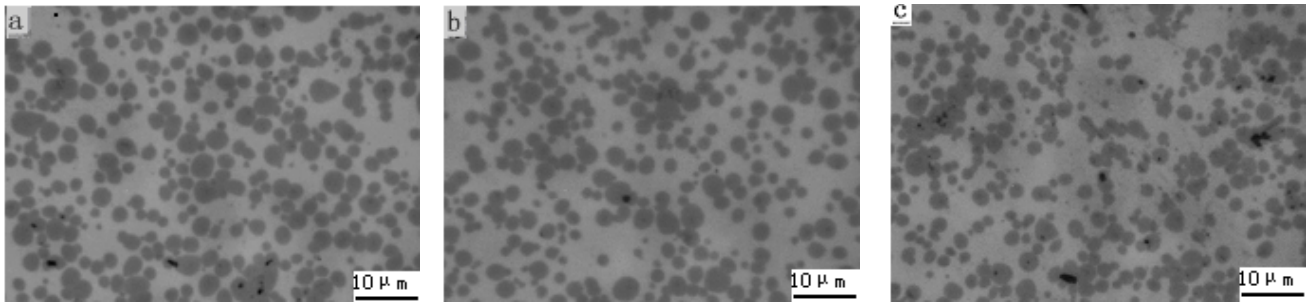


Fig. 4. Microstructures of Fe-VC composite at different sintering temperature: a – 1493 K; b – 1473 K; c – 1433 K

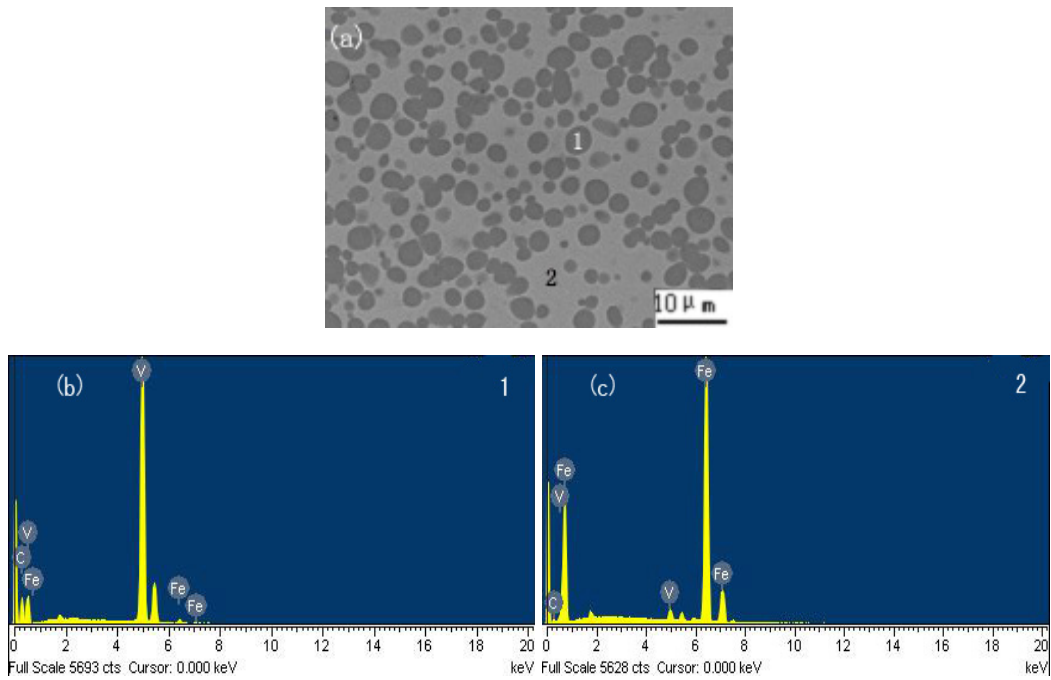


Fig. 5. Microstructure of Fe-VC composites sintered at 1473 K – (a); corresponding EDS spectrums – (b) and (c)

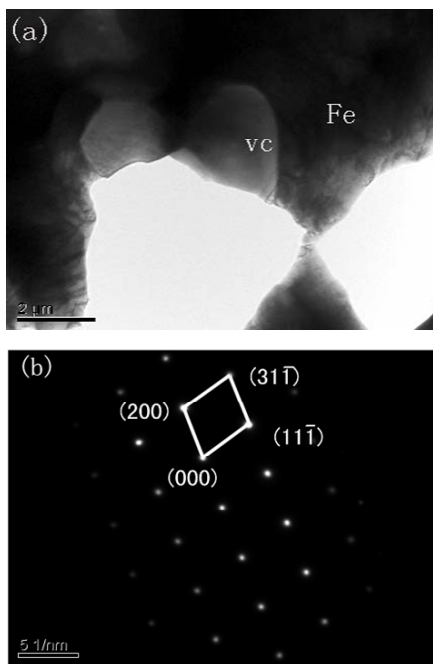


Fig. 6. TEM micrograph of the Fe-VC composite (a); the elected diffraction pattern of VC (b)

Table 2. Bending strength of Fe-VC composite

	σ_F (MPa)
Longitudinal direction	1401.27
Transverse direction	1384.63

lighter region are estimated as VC and Fe matrix by the EDS (see Fig. 5, b and c). It can be found that the spherical VC particles homogeneously distribute in iron matrix with particle size in the range 1 μm –5 μm , which is beneficial to ensure mechanical properties of Fe-VC composite are isotropic and stress distribution is uniform in Fe-VC composite. As shown in Table 2, the bending strength of Fe-VC composite in different direction justifies its isotropy. Further TEM investigation of the Fe-VC composite sintered at 1473 K is made and the result is shown in Fig. 6. The clean interface between VC reinforcement and the iron matrix can be observed, and any interface precipitates don't be found. As a result, the strong interface bond can be obtained, which is favorable to the mechanical properties of Fe-VC composite. In addition, no interface separation between VC reinforcement and iron matrix is found in Fe-VC composite. Therefore, wettability of iron matrix with VC

particles is good, which is great importance of structure and mechanical properties for Fe-VC composite [20].

Table 3. Wear weight loss of Fe-VC composite and hardened 1045 steel

	Hardness (HRC)	Wear weight loss (mg)
Hardened 1045 steel	55	13.4
Fe-VC composite sintered at 1473K	58	1.2

3. 3. Wear properties of Fe-VC composite

The wear weight loss of Fe-VC composite sintered at 1473 K and the hardened 1045 steel is shown in Table 3. It can be found that Fe-VC composite possesses great wear-resistance, being 11.1-times that of the hardened 1045 steel.

The SEM micrographs of the wear surfaces of hardened 1045 steel and Fe-VC composite sintered at 1473 K are shown in Fig. 7. Obviously, the grooves can be observed in wear surfaces. The reasons that the formation of grooves are as follows: the load applied between the pin and the disk can be divided into two parts in dry sliding abrasive wear tests: normal stress and shear stress. The normal stress makes the Al_2O_3 abrasive particles penetrate the surfaces of hardened 1045 steel and Fe-VC composite, and the shear stress makes the Al_2O_3 abrasive particles plough the surfaces of hardened 1045 steel and Fe-VC composite in tangential direction. As a result, the Al_2O_3 abrasive particles eventually remove or push the materials into ridges along sides of the grooves [21]. In addition, the grooves are much shallower in Fe-VC composite than that of the hardened 1045 steel, which is owing to high hardness VC particles in Fe-VC composite effectively reinforcing the iron matrix and protecting it from serious abrasion.

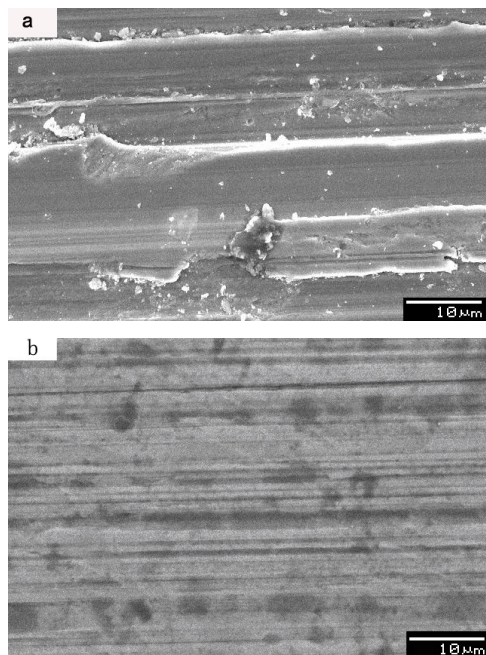


Fig. 7. SEM micrographs of wear surfaces: a – hardened 1045 steel; b – Fe-VC composite

4. CONCLUSIONS

Bulk Fe-VC composite is prepared by a process which is regarded as the combination of in situ synthesis technique and powder metallurgy technique. VC reinforcement is generated through the reaction: $FeV + C = VC + Fe$.

The microstructure of the composite reveals that the fine VC particulates distribute evenly in iron matrix; the VC/matrix interface is defect free; and interface debonding is not observed in Fe-VC composite.

The dry-sliding abrasive wear test indicates that Fe-VC composite possesses great wear resistance, being 11.1 times than that of the hardened 1045 steel.

Acknowledgement

This research was supported by the grant from the Science & Technology Department of Sichuan Province (2011JY0041), Sichuan Provincial Education Department (13ZB0047), Chongqing Pingwei Science and Technology Group Co.,Ltd. (K11031).

REFERENCES

1. **Dogan, O.-N., Hawk, J.-A., Tylczak, J.-H.** Wear of Titanium Carbide Reinforced Metal Matrix Composites *Wear* 225 1999: pp. 758–796.
2. **Dogan, O.-N., Hawk, J.-A., Tylczak, J.-H.,** Wear of Cast Chromium Steels with TiC Reinforcement *Wear* 250 2001: pp. 462–469.
3. **Varol, T., Canakci, A.,** Effect of Particle Size and Ratio of B_4C Reinforcement on Properties and Morphology of Nanocrystalline $Al_{2024}-B_4C$ Composite Powders *Powder Technology* 246 2013: pp. 462–472. <http://dx.doi.org/10.1016/j.powtec.2013.05.048>
4. **Varol, T., Canakci, A.,** Synthesis and Characterization of Nanocrystalline $Al_{2024}-B_4C$ Composite Powders by Mechanical Alloying *Philosophical Magazine Letters* 93 2013: pp. 339–345.
5. **Varol, T., Canakci, A.** Effect of Weight Percentage and Particle Size of B_4C Reinforcement on Physical and Mechanical Properties of Powder Metallurgy $Al_{2024}-B_4C$ Composites *Metals and Materials International* 19 2013: pp. 1227–1234.
6. **Varol, T., Canakci, A., Ozsahin, S.** Artificial Neural Network Modeling to Effect of Reinforcement Properties on the Physical and Mechanical Properties of $Al_{2024}-B_4C$ Composites Produced by Powder Metallurgy *Composites: Part B* 54 2013: pp. 224–233. <http://dx.doi.org/10.1016/j.compositesb.2013.05.015>
7. **Canakci, A., Arslan, F., Varol, T.** Effect of Volume Fraction and Size of B_4C Particles on Production and Microstructure Properties of B_4C Reinforced Aluminum Alloy Composites *Materials Science and Technology* 29 2013: pp. 954–960. <http://dx.doi.org/10.1179/1743284713Y.0000000232>
8. **Wang, Y.-S., Zhang, X.-Y., Zeng, G.-T., Li, F.-C.** Study on an Fe-TiC Surface Composite Produced in situ *Materials & Design* 20 1999: pp. 233–236. [http://dx.doi.org/10.1016/S0261-3069\(98\)00049-1](http://dx.doi.org/10.1016/S0261-3069(98)00049-1)
9. **Das, K., Bandyopadhyay, T.-K.** Effect of Form of Carbon on the Microstructure of in situ Synthesized TiC-reinforced Iron-based Composite *Materials Letters* 58 2004: pp. 1877–1880. <http://dx.doi.org/10.1016/j.matlet.2003.11.034>

10. **Zhang, X.-N., Lü, W.-J., Zhang, D., Wu, R.-J.** In situ Technique for Synthesizing (TiB + TiC)/Ti Composites *Scripta Materialia* 41 1999: pp. 39–46.
[http://dx.doi.org/10.1016/S1359-6462\(99\)00087-1](http://dx.doi.org/10.1016/S1359-6462(99)00087-1)
11. **Raghunath, C., Bhat, M.-S., Rohagi, P.-K.** In situ Technique for Synthesizing Fe-TiC Composites *Scripta Metallurgica et Materialia* 4 1995: pp. 577–582.
[http://dx.doi.org/10.1016/0956-716X\(95\)90840-G](http://dx.doi.org/10.1016/0956-716X(95)90840-G)
12. **Terry, B.-S., Chinyamakobvu, O.-S.** In situ Production of Fe-TiC Composites by Reaction in Liquid Iron Alloy *Journal of Materials Science Letters* 10 1991: pp. 628–629.
13. **Akhtar, F.** Microstructure Evolution and Wear Properties of in situ Synthesized TiB₂ and TiC Reinforced Steel Matrix Composites *Journal of Alloys and Compounds* 459 2008: pp. 491–497.
<http://dx.doi.org/10.1016/j.jallcom.2007.05.018>
14. **Wang, X.-H., Zhang, M., Liu, X.-M., Qu, S.-Y., Zou, Z.-D.** Microstructure and Wear Properties of TiC/FeCrBSi Surface Composite Coating Prepared by Laser Cladding *Surface and Coatings Technology* 202 2008: pp. 3600–3606.
15. **Wang, Y.-S., Li, F.-C., Zeng, G.-T., Feng, D.-L.** Structure And Wear-Resistance Of An Fe-VC Surface Composite Produced in situ *Materials & Design* 20 1999: pp. 19–22.
[http://dx.doi.org/10.1016/S0261-3069\(98\)00033-8](http://dx.doi.org/10.1016/S0261-3069(98)00033-8)
16. **Wang, Y.-S., Zhang, X.-Y., Zeng, G.-T., Li, F.-C.** In situ Production of Fe-VC and Fe-TiC Surface Composites by Cast-sintering *Composites Part A* 32 2001: pp. 281–286.
17. **Wang, J., Wang, Y.-S., Ding, Y.-C.** Production of (Ti,V)C Reinforced Fe Matrix Composites *Materials Science and Engineering A* 454–455 2007: pp. 75–79.
18. **Oliveira, M.-M., Bolton, J.-D.** High-speed Steels: Increasing Wear Resistance by Adding Ceramic Particles *Journal of Materials Processing Technology* 92–93 1999: pp. 15–20.
19. **Patril, P., Anders, E.-W., Steven, S.** Self-propagating High-temperature Synthesis and Liquid-phase Sintering of TiC/Fe Composites *Journal of Materials Processing Technology* 127 2002: pp. 131–139.
[http://dx.doi.org/10.1016/S0924-0136\(02\)00113-9](http://dx.doi.org/10.1016/S0924-0136(02)00113-9)
20. **Farid, A., Guo, S.** TiB₂ and TiC Stainless Steel Matrix Composites *Materials Letters* 61 2007: pp. 189–191.
<http://dx.doi.org/10.1016/j.matlet.2006.04.028>
21. **Liu, Y.-F., Mu, J.-S., Xu, X.-Y., Yang, S.-Z.** Microstructure and Dry-sliding Wear Properties of TiC-reinforced Composite Coating Prepared by Plasma-transferred arc Weld-surfacing Process *Materials Science and Engineering A* 458 2007: pp. 366–370.
<http://dx.doi.org/10.1016/j.msea.2006.12.086>